HHS Public Access

Author manuscript

Circ Res. Author manuscript; available in PMC 2017 June 10.

Published in final edited form as:

Circ Res. 2016 June 10; 118(12): 1918–1929. doi:10.1161/CIRCRESAHA.116.308688.

Deletion of Interleukin-6 Attenuates Pressure Overload-Induced Left Ventricular Hypertrophy and Dysfunction

Lin Zhao[#1,2], **Guangming Cheng**[#2], **Runming Jin**[#1], **Muhammad R. Afzal**[2], **Anweshan Samanta**[2], **Yu-Ting Xuan**[2], **Magdy Girgis**[2], **Harold K Elias**[3], **Yanqing Zhu**[2], **Arash Davani**[2], **Yanjuan Yang**[2], **Xing Chen**[2], **Sheng Ye**[2], **Ou-Li Wang**[2], **Lei Chen**[2], **Jeryl Hauptman**[2], **Robert J. Vincent**[2], and **Buddhadeb Dawn**[2]

[1]Department of Pediatrics, Union Hospital, Tongji Medical College, Huazhong University of Science and Technology, Wuhan, Hubei, China

[2]Division of Cardiovascular Diseases, Cardiovascular Research Institute, University of Kansas Medical Center, Kansas City, KS

[3]Mount Sinai School of Medicine, New York, NY.

[#] These authors contributed equally to this work.

Abstract

Rationale—The role of interleukin (IL)-6 in the pathogenesis of cardiac myocyte hypertrophy remains controversial.

Objective—To conclusively determine whether IL-6 signaling is essential for the development of pressure overload-induced left ventricular (LV) hypertrophy, and to elucidate the underlying molecular pathways.

Methods and Results—Wild-type (WT) and *IL-6* knockout ($IL\text{-}6^{-/-}$) mice underwent sham surgery or transverse aortic constriction (TAC) to induce pressure overload. Serial echocardiograms and terminal hemodynamic studies revealed attenuated LV hypertrophy and superior preservation of LV function in $IL\text{-}6^{-/-}$ mice after TAC. The extents of LV remodeling, fibrosis, and apoptosis were reduced in $IL\text{-}6^{-/-}$ hearts after TAC. Transcriptional and protein assays of myocardial tissue identified CaMKII and STAT3 activation as important underlying mechanisms during cardiac hypertrophy induced by TAC. The involvement of these pathways in myocyte hypertrophy was verified in isolated cardiac myocytes from WT and $IL\text{-}6^{-/-}$ mice exposed to pro-hypertrophy agents. Furthermore, overexpression of CaMKII in H9c2 cells increased STAT3 phosphorylation, and exposure of H9c2 cells to IL-6 resulted in STAT3 activation that was attenuated by CaMKII inhibition. Together these results identify the importance of CaMKII-dependent activation of STAT3 during cardiac myocyte hypertrophy via IL-6 signaling.

Address correspondence to: Dr. Buddhadeb Dawn, Division of Cardiovascular Diseases, 3901 Rainbow Boulevard, 1001 Eaton, MS 3006, Kansas City, KS 66160, Tel: 913-588-6015, Fax: 913-588-6010, bdawn@kumc.edu.

DISCLOSURES

None.

Conclusions—Genetic deletion of *IL-6* attenuates TAC-induced LV hypertrophy and dysfunction, indicating a critical role played by IL-6 in the pathogenesis of LV hypertrophy in response to pressure overload. CaMKII plays an important role in IL-6-induced STAT3 activation and consequent cardiac myocyte hypertrophy. These findings may have significant therapeutic implications for LV hypertrophy and failure in patients with hypertension.

Keywords

Interleukin-6; left ventricular hypertrophy; cardiac myocyte; Ca^{2+}/calmodulin-dependent protein kinase II; signal transducer and activator of transcription 3

INTRODUCTION

Millions of patients worldwide suffer from hypertension and its cardiovascular sequelae, left ventricular (LV) hypertrophy and congestive heart failure. The spectrum of hypertensive heart disease directly or indirectly accounts for inordinate morbidity and mortality globally. Although several signaling pathways have been known to influence cardiac myocyte hypertrophy, the precise molecular pathogenesis of LV hypertrophy and failure in response to pressure overload remains unclear.

Interleukin (IL)-6, an inflammatory cytokine with pleiotropic effects in diverse cells and organs, has been implicated in cardiovascular pathologies.[1,2] IL-6 is produced by cardiac myocytes themselves, and persistent activation of gp130, a key component of IL-6 signaling, induced myocardial hypertrophy in mice.[3] However, gp130 also transduces signaling by other members of the IL-6 family of cytokines, and hence not specific for IL-6. A subsequent study has shown that IL-6 infusion results in concentric hypertrophy in rats, albeit without increasing blood pressure.[4] However, there is no direct evidence to date that IL-6 signaling is necessary for pressure overload-induced LV hypertrophy.

Interestingly, and contrary to the notion that IL-6 signaling is critical for cardiac myocyte hypertrophy, in a study using *IL-6*$^{-/-}$ mice, Kaminski and colleagues concluded that IL-6 was not necessary for cardiac hypertrophy in mice.[5] Furthermore, using a model of transverse aortic constriction (TAC), Lai and colleagues reported similar LV hypertrophy, dilation and dysfunction in control and *IL-6*$^{-/-}$ mice, indicating that IL-6 was not essential for pressure overload-induced hypertrophy in vivo.[6]

Considering the above controversies, and the well-known association of IL-6 with cardiovascular pathologies, we sought to conclusively determine whether IL-6 is necessary for pressure overload-induced hypertrophy using an *in vivo* model of TAC. We also elucidated the molecular pathways involved in this process. Our results indicate that pressure overload-induced deleterious effects on LV structure and function are attenuated in the absence of IL-6, indicating an essential role played by this cytokine. Our molecular data further unravel several heretofore unknown signaling roles, including the contribution of Ca^{2+}/calmodulin-dependent protein kinase II (CaMKII) toward signal transducer and activator of transcription 3 (STAT3) activation in this process.

METHODS

An expanded methods section is available in the Online Data Supplement.

Animals

All animal experiments were performed in accordance with the guidelines of the Institutional Animal Care and Use Committee at the University of Kansas Medical Center. Male *IL-6*$^{-/-}$ mice (*IL-6*^{tm1Kopf}, genetic background C57BL/6J, stock No: 002650) were purchased from the Jackson Laboratory (Bar Harbor, ME). Age and body weight-matched wild-type C57BL/6J mice (WT) were used as controls. Deletion of *IL-6* was confirmed by PCR using mouse tail genomic DNA as template (Online Figure I).

Minimally invasive transverse aortic constriction

Minimally invasive transverse aortic constriction was performed to induce left ventricular (LV) pressure overload in age- and body weight-matched mice.

Histology

Standard methods were used for the assessment of fibrosis and apoptosis.

Measurement of cardiac myocyte size

cardiac myocytes were isolated from WT and *IL-6*$^{-/-}$ mice at 6 weeks after sham and TAC procedures.

Echocardiography

LV function and structure were assessed by serial transthoracic echocardiography prior to surgery and at 1, 2, 4, and 6 weeks after surgery using published methods.[7,8]

Invasive hemodynamic studies

Open chest in vivo hemodynamic studies were performed.[7]

Assessment of apoptosis

Myocyte apoptosis was quantitated using Terminal dUTP Nick End-labeling (TUNEL) assay performed on myocardial sections at 6 weeks after TAC.

H9c2 myoblast culture

H9c2 cells were maintained according to suggested culture methods. Transfection of H9c2 cells was performed using Lipofectamine 2000 (Invitrogen, Carlsbad, CA) and plasmids targeting CaMKII (Addgene, Cambridge, MA).

Cell treatments

Isolated adult cardiac myocytes were stimulated with angiotensin II (Ang II), phenylephrine (PE) or recombinant IL-6 (rIL-6); H9c2 myoblasts were exposed to rIL-6, and CaMKII or STAT3 inhibitors.

Assessment of cell surface area

H9c2 cells were fixed with 4% paraformaldehyde and stained with 1% crystal violet for assessment of cell surface area.

Quantitative PCR

Total RNA was isolated from frozen tissues and cultured cells and processed for real-time quantitative reverse transcription polymerase chain reaction (qPCR) using standard protocols.

Protein extraction and western blot analysis

Standardized protocols were used as described in the Online Data Supplement.

Statistical analysis

Data were expressed as mean ± SEM. For comparison of 2 groups, Student's *t* tests (2-tailed) were performed; multiple groups (≥ 3groups) comparison was performed by one-way ANOVA with Bonferroni's *post hoc* test. Serial echocardiographic parameters were analyzed using two-way (time and group) ANOVA followed by Student's *t* tests with the Bonferroni correction. *P* values less than 0.05 were considered statistically significant. All statistical analyses were performed using the SPSS software version 22.0 (IBM, Armonk, NY).

RESULTS

Experimental protocol

The *in vivo* experimental protocol is summarized in Online Figure II. A total of 153 mice were enrolled. Fifteen mice were excluded for the reasons specified in Online Table II. Following a baseline echocardiography, WT and *IL-6*$^{-/-}$ mice underwent either TAC (TAC group) or sham (sham group) surgery. Echocardiography was repeated at 1, 2, 4 and 6 weeks after the surgery for quantitative assessment of LV structural and functional parameters. Mice were sacrificed at 6 weeks after surgery following a terminal hemodynamic study. Histological and molecular assays were performed utilizing myocardial tissue harvested at 1, 2 and 6 weeks after surgery. *In vitro* experiments were conducted using cardiac myocytes isolated from WT and *IL-6*$^{-/-}$ hearts after TAC.

Genetic deletion of IL-6 attenuated LV hypertrophy induced by pressure overload in vivo

Gross morphology after 6 weeks of surgery in the WT and *IL-6*$^{-/-}$ mice (Figure 1A) suggested attenuation of hypertrophy in *IL-6*$^{-/-}$ hearts. We used heart weight/tibia length (HW/TL) ratio to assess changes in LV mass. As expected, HW/TL in sham-operated WT and *IL-6*$^{-/-}$ mice were similar. However, in the TAC groups, HW/TL in WT mice was significantly higher compared with *IL-6*$^{-/-}$ mice (10.1 ± 0.44mg/mm vs. 8.8 ± 0.29mg/mm, $P<0.05$) (Figure 1B; Online Table III). Next, we measured the cross-sectional area of myocytes in both groups. Interestingly, myocytes in sham-operated *IL-6*$^{-/-}$ hearts at 6 weeks after TAC were smaller compared with WT counterparts (135.1 ± 13.2μm^2 vs. 167.4 ± 6.7μm^2, $P<0.05$) (Figure 1C; Online Table IV). These findings suggest that IL-6 plays an important role in the normal development of cardiac myocytes. After TAC, the transverse

area of myocytes increased in both WT and *IL-6*$^{-/-}$ mice; however, this increase was significantly attenuated in *IL-6*$^{-/-}$ mice compared with WT mice (173.4 ± 12.3μm^2 vs. 256.4 ± 17.7μm^2, $P<0.05$) (Figure 1C; Online Table IV). Due to differences in the transverse area of myocytes in *IL-6*$^{-/-}$ and WT mice in the sham group, we calculated the percent change in the area in respective TAC group. The increase in myocyte area in WT mice was significantly greater compared with *IL-6*$^{-/-}$ mice (53% vs. 28%, $P<0.05$). These results indicate that the absence of IL-6 attenuates LV hypertrophy induced by pressure overload.

In addition, we measured surface area of cardiac myocytes isolated from WT and *IL-6*$^{-/-}$ mice at 6 weeks after surgery. Consistent with histological observations above, cardiac myocytes isolated from *IL-6*$^{-/-}$ mice were smaller than WT in the sham group (3126.78 ± 73.33 μm^2 vs. 3415.11 ± 60.56 μm^2, $P<0.05$) (Figure 1D,E). Cell surface area increased in both WT and *IL-6*$^{-/-}$ mice after TAC, however, the increase was significantly attenuated in *IL-6*$^{-/-}$ myocytes compared with WT (3904.30 ± 21.24μm^2 vs. 5208.14 ± 243μm^2, $P<0.05$) (Figure 1D,E). Similarly, the width of isolated cardiac myocytes was less in *IL-6*$^{-/-}$ mice compared with WT in the sham groups (20.9 ± 0.32μm vs.22.9 ± 0.25 μm, $P<0.05$) (Figure 1D,F); and the increase in myocyte width was significantly attenuated in *IL-6*$^{-/-}$ mice compared with WT mice (23.96 ± 0.09μm vs. 26.14 ± 0.61μm, $P<0.05$) (Figure 1D,F) in the TAC groups. Interestingly, there was no difference in length between WT and *IL-6*$^{-/-}$ myocytes in the sham groups (145.5 ± 1.56μm vs. 143.7 ± 2.8μm, *P=NS*) (Figure 1G). There was an increase in cardiac myocyte length in the TAC groups; however, the increase was significantly attenuated in *IL-6*$^{-/-}$ hearts compared with WT hearts (169.78 ± 0.83μm vs. 191.93 ± 5.38μm, $P<0.05$) (Figure 1G).

To confirm findings at the molecular level, we performed mRNA and protein characterization for hypertrophy-related markers using tissue samples isolated at 2 weeks after surgery. There was significantly higher mRNA expression of atrial natriuretic peptide (*anp*), brain natriuretic peptide (*bnp*), alpha skeletal muscle actin (*α-SK actin*) and GATA binding protein 4 (*gata4*) in WT hearts compared with *IL-6*$^{-/-}$ hearts after TAC. There was no significant difference between sham-operated WT and *IL-6*$^{-/-}$ hearts (Figure 1H). Consistently, protein expression for ANP was significantly higher in WT hearts compared with *IL-6*$^{-/-}$ hearts at both 2 and 6 weeks after TAC (Figure 1I,J). The continued suppression of ANP in *IL-6*$^{-/-}$ mice at 6 weeks after TAC suggests that the protective effect of IL-6 deletion is sustained.

Pressure overload-induced ventricular remodeling was ameliorated in the absence of IL-6

Echocardiographic LV mass increased in both WT and *IL-6*$^{-/-}$ mice at 1 week after TAC; however, the increase was significantly greater in WT mice (101.77 ± 4.87mg vs. 88.79 ± 3.51mg, $P<0.05$) (Figure 2A). The other parameters of LV remodeling including posterior wall thickness at end-diastole, LV end-diastolic diameter (LVEDD) and LV end-diastolic volume (LVEDV) were also significantly persevered in *IL-6*$^{-/-}$ mice compared with WT mice after TAC (Figure 2B-D). The LV chamber diameter measured in hearts harvested at 6 weeks after surgery was significantly larger in WT compared with *IL-6*$^{-/-}$ mice in the TAC groups (4.2 ± 0.05mm vs. 3.8 ± 0.05mm, $P<0.05$) (Figure 2E). These results corroborated with the echocardiographic data.

Genetic deletion of IL-6 prevented pressure overload-induced LV dysfunction

There was no significant difference in LV ejection fraction (LVEF) (69.11% ± 1.06% vs. 70.56% ± 0.92%, in WT and *IL-6*$^{-/-}$ mice, respectively, *P*=NS; Figure 3A) and LV fractional shortening (LVFS) (39.81% ± 0.98% vs. 39.21% ± 2.06%, in WT and *IL-6*$^{-/-}$ mice, respectively, *P*=NS; Figure 3B) at baseline. LVEF decreased in both WT and *IL-6*$^{-/-}$ mice at 1 week after TAC; however, the reduction was significantly greater in WT mice compared with *IL-6*$^{-/-}$ mice (64.21% ± 0.83% vs. 66.77% ± 0.64%, *P*<0.05; Figure 3A). Similar results were noted for LVFS in the TAC group (35.42% ± 0.72% vs. 37.69% ± 0.70%, *P*<0.05; Figure 3B). There was continued reduction in LVEF and LVFS in WT mice during follow-up at 2, 4 and 6 weeks after TAC. At each follow-up time point, cardiac function was better preserved in *IL-6*$^{-/-}$ mice compared with WT mice (Figure 3A,B). Consistently, the progressive increase in LV end-systolic volume (LVESV) was also less pronounced in *IL-6*$^{-/-}$ mice (Figure 3C).

These observations corroborated with data from invasive hemodynamic studies at 6 weeks after surgery. LV dP/dt_{max} was significantly better in *IL-6*$^{-/-}$ mice compared with WT mice in the TAC groups, while there was no significant difference in the sham groups (Figure 3D; Online Table V). The end-systolic pressure-volume relationship (ESPVR) also showed preserved systolic function in *IL-6*$^{-/-}$ mice compared with WT mice in the TAC groups (Figure 3E,F; Online Table V). The parameters of LV diastolic function, including dP/dt_{min} and Tau (τ) showed superior preservation of diastolic function in *IL-6*$^{-/-}$ mice compared with WT mice (Figure 3G,H; Online Table V). Finally, LV end-diastolic pressure (LVEDP) was also lower in *IL-6*$^{-/-}$ mice compared with WT mice in the TAC groups (Figure 3I; Online Table V).

Pressure overload-induced myocardial fibrosis was attenuated in IL-6$^{-/-}$ hearts

Myocardial interstitial and perivascular fibrosis was assessed in picrosirius red-stained sections at 6 weeks after surgery. There was no significant difference in the extents of interstitial and perivascular fibrosis in WT and *IL-6*$^{-/-}$ mice in the sham groups. However, both interstitial and perivascular fibrosis increased in WT hearts after TAC, with more pronounced changes in perivascular areas (Figure 4A-D). This increase in interstitial and perivascular fibrosis was significantly blunted in *IL-6*$^{-/-}$ hearts after TAC (Figure 4A-D). To understand the molecular underpinnings of these results, we assessed gene and protein expression of fibrosis-related molecules in myocardial tissue. The mRNA levels for collagen type I alpha 1 (Col1A1), collagen type III alpha 1 (Col3A1) and periostin were measured in LV tissue samples harvested at 2 weeks after surgery. Consistent with data from quantitative analysis of fibrosis in picrosirius red-stained myocardial sections, the mRNA expression for Col1A1 and Col3A1 was significantly higher in WT compared with *IL-6*$^{-/-}$ mice after TAC (Figure 4E). The mRNA expression of periostin was also significantly higher in WT compared with *IL-6*$^{-/-}$ mice after TAC (Figure 4E). The TAC-induced increase in myocardial periostin expression was also confirmed at the protein level (Figure 4F). Importantly, increased expression of MMP9 noted in WT hearts at 6 weeks after TAC was attenuated in *IL-6*$^{-/-}$ hearts (Figure 4F). These results from mRNA and protein characterization were consistent with our histological findings of improved remodeling in the absence of IL-6.

Genetic deletion of IL-6 attenuated cardiac myocyte apoptosis induced by pressure overload

To elucidate the role of IL-6 in the pressure overload-induced apoptosis, we performed TUNEL staining on myocardial samples harvested at 6 weeks after surgery. The percentage of apoptotic cardiac myocyte nuclei in WT hearts was significantly greater than *IL-6*$^{-/-}$ hearts in the TAC groups (0.074±0.012% vs. 0.040±0.008%, $P<0.05$; Figure 5A,B), indicating that absence of IL-6 protects cardiac myocytes from pressure overload-induced apoptosis. Consistent with these observations, the expression of proapoptotic molecule Bcl-2-assocaited X protein (Bax) in WT hearts was greater compared with *IL-6*$^{-/-}$ hearts at 6 weeks after TAC. Moreover, the levels of antiapoptotic molecule Bcl-2 were reduced in WT hearts compared with *IL-6*$^{-/-}$ hearts at 6 weeks after TAC (Figure 5C). The ratio of Bax/Bcl-2 was significantly lower in *IL-6*$^{-/-}$ hearts compared with WT hearts in TAC groups (Figure 5D), suggesting that the absence of IL-6 promotes an antiapoptotic milieu.

Hypertrophic response was attenuated in IL-6$^{-/-}$ adult cardiac myocytes

To specifically examine the role of IL-6 in cardiac myocyte hypertrophy, we performed *in vitro* experiments using cardiac myocytes isolated from WT and *IL-6*$^{-/-}$ mice. These cardiac myocytes were exposed to rIL-6 for 24 h followed by isolation of mRNA and quantitative PCR for hypertrophy related genes (*anp, bnp* and *myh-7*). The expression of these genes after rIL-6 stimulation was significantly higher in WT cardiac myocytes compared with *IL-6*$^{-/-}$ cardiac myocytes (Figure 6A). This prompted us to explore the expression of IL-6 receptors in WT and *IL-6*$^{-/-}$ cardiac myocytes. Indeed, the expression of IL-6 receptors was lower in *IL-6*$^{-/-}$ cardiac myocytes compared with WT cardiac myocytes (Figure 6B), offering a possible explanation for the lack of response to IL-6. Next, we tested the effects of Ang II on cardiac myocytes isolated from WT and *IL-6*$^{-/-}$ mice. Although Ang II increased the expression of *anp, bnp* and *myh-7* in both groups, the response was blunted in *IL-6*$^{-/-}$ cardiac myocytes (Figure 6C). When WT and *IL-6*$^{-/-}$ cardiac myocytes were stimulated with PE, another hypertrophy-promoting agent, the results showed similar trends (Figure 6D). Together, these results corroborate our *in vivo* observations regarding the requirement of IL-6 for pressure overload-induced cardiac hypertrophy.

Pressure overload-induced activation of MAPK and Akt signaling pathways was suppressed by genetic deletion of IL-6

Since mitogen-activated protein kinase (MAPK) pathways are involved in gp130-mediated cardiac myocyte hypertrophy,[9] we assessed the levels of phosphorylated ERK1/2 and JNK at 6 weeks after surgery. Although phosphorylated ERK1/2 increased in both WT and *IL-6*$^{-/-}$ mice after TAC, the increase was attenuated in *IL-6*$^{-/-}$ mice (Online Figure IIIA,B), indicating that intact IL-6 signaling is necessary for pressure overload-induced activation of ERK1/2. Similarly, the increase in phosphorylated JNK levels noted in WT hearts after TAC was attenuated in *IL-6*$^{-/-}$ hearts (Online Figure IIIA,C), albeit the difference was less pronounced. In addition, increased phosphorylation of Akt (Online Figure IIID,E) and GSK-3β (Online Figure IIID,F) was noted in WT hearts after TAC; both of which were significantly attenuated in *IL-6*$^{-/-}$ hearts. There was no significant difference in the levels of these proteins in sham-operated WT and *IL-6*$^{-/-}$ mice (Online Figure IIIA-F).

CaMKII and STAT3 contributed to IL-6-induced cardiac myocyte hypertrophy

Previous studies have suggested the involvement of STAT3[10] and CaMKII[11] in pressure overload-induced cardiac hypertrophy. At 6 weeks after TAC, the levels of phosphorylated STAT3 (pTyr-STAT) and phosphorylated CaMKII (p-CaMKII) increased in both WT and *IL-6*$^{-/-}$ mice; however, the increase was significantly attenuated in *IL-6*$^{-/-}$ mice (Figure 7A-C). These observations highlight a significant role of IL-6 signaling in phosphorylation of STAT3 and CaMKII in specifically in the setting of TAC-induced hypertrophy. To further confirm the interaction of IL-6 signaling with STAT3 and CaMKII, we used rIL-6 for stimulation of H9c2 myoblasts in the presence and absence of inhibitors of STAT3 and CaMKII. Exposure to rIL-6 increased the surface area of H9c2 cells indicating hypertrophy; however, this increase was blocked in the presence of STAT3 inhibitor as well as CaMKII inhibitor (Figure 7D,E). Consistently, exposure to rIL-6 also increased gene expression of hypertrophy markers (*anp, bnp*) in H9c2 cells; and this was suppressed in the presence of STAT3 and CaMKII inhibitors (Figure 7F). To understand the time-dependent nature of phosphorylation of STAT3 and CaMKII, we treated H9c2 cells with rIL-6 for variable durations. IL-6-induced phosphorylation of STAT3 and CaMKII peaked in 30 min and plateaued subsequently (Figure 7G-I). Our observations indicate that phosphorylation of CaMKII and STAT3 follow a similar time-course after exposure to IL-6. Together, these data from harvested tissues and H9c2 cells identify important roles of CaMKII and STAT3 in IL-6-induced cardiac hypertrophy.

IL-6 activated STAT3 via a CaMKII-dependent manner

The relationship between CaMKII and STAT3 activation was further investigated by transiently transfecting H9c2 cells with a vector encoding CaMKII. H9c2 cells transfected with an empty vector served as controls. The levels of CaMKII, p-CaMKII and pTyr-STAT3 increased significantly in CaMKII-transfected cells 48 h later, suggesting that CaMKII may be an upstream activator of STAT3 (Figure 8A-C). This relationship was further confirmed by using an inhibitor of CaMKII (KN-62) prior to stimulation of H9c2 cells with rIL-6. The level of pTyr-STAT3 was significantly attenuated in the presence of CaMKII inhibitor (Figure 8D-F). Since STAT3 is translocated to the nucleus following phosphorylation, we examined phosphorylated protein levels in cytoplasmic and nuclear fractions. pTyr-STAT3 levels increased significantly in both fractions in H9c2 cells treated with rIL-6. However, the addition of CaMKII inhibitor resulted in significant reduction in pTyr-STAT3 levels in both nuclear and cytoplasmic fractions of rIL-6-exposed cells (Figure 8G-I). Taken together, these observations confirm that CaMKII is upstream of STAT3 and plays important role in the activation of STAT3 by IL-6. Similar experiments using isolated adult cardiac myocytes yielded similar results (Online Figure IV) further confirming the role of CaMKII in IL-6-induced STAT3 activation.

DISCUSSION

Salient findings

Newer therapeutic approaches are urgently needed to improve the clinical outcomes in millions of patients with hypertensive heart disease. However, and despite intense research, the precise molecular pathways that can be modulated to prevent LV hypertrophy remain

poorly understood. In particular, the involvement of IL-6, an inflammatory cytokine, in this process remains controversial. Our studies using a mouse model of pressure overload *in vivo* and isolated cardiac myocytes *in vitro* provide the following important observations: i) genetic deletion of *IL-6* attenuates pressure overload-induced cardiac hypertrophy; ii) pressure overload-induced LV remodeling and dysfunction are ameliorated in the absence of IL-6, indicating a critical role of this cytokine in the pathogenesis of these unfavorable outcomes; iii) pressure overload-induced myocardial fibrosis and apoptosis are ameliorated in the absence of *IL-6*; iv) IL-6 is required for hypertrophy of adult cardiac myocytes in response to Ang II and PE; and v) CaMKII plays a heretofore unknown and important role in IL-6-induced STAT3 activation and cardiac myocyte hypertrophy. These signaling insights may be useful toward formulation of novel cardioprotective strategies in hypertensive patients.

IL-6 deletion prevents LV hypertrophy in response to pressure overload

Although gp130, a key component of IL-6 signaling, and the IL-6 family of cytokines collectively have been implicated in LV hypertrophy, the specific impact of IL-6 signaling with regard to LV hypertrophy remains unsubstantiated and controversial. Importantly, gp130 transduces signaling not only for IL-6, but also for the other members of this family of cytokines. As for IL-6 specifically, previous studies have shown that hypertrophy induced by AngII and norepinephrine (NE) is significantly attenuated in *IL-6*$^{-/-}$ mice suggesting a role of IL-6 in pathological hypertrophy.[12,13] A previous study in rats showed that IL-6 infusion for 7 days induced LV hypertrophy, albeit without raising blood pressure.[4] The direct impact of *IL-6* deletion on pressure overload-induced LV hypertrophy has been investigated to date only in one study, which showed no effect of *IL-6* deletion on pressure overload-induced LV dysfunction and remodeling at 2 and 4 weeks after TAC.[6]

Using a similar model of TAC, our study is the first to report that genetic deletion of *IL-6* prevents LV hypertrophy, thereby identifying a critical role of this cytokine in the pathogenesis of hypertensive heart disease. The potential reasons for differences between observations made by Lai and colleagues[6] and our current findings include possible differences in the severity of TAC and the differences in follow-up durations. In the study by Lai et al., mice were followed for 4 weeks after TAC, while our observations were made at 6 weeks after TAC. Although it is possible that the protective effects of *IL-6* deletion become more pronounced with longer follow-up after TAC, the duration of follow-up may not be the primary reason for the observed differences, because the benefits of *IL-6* deletion were apparent even at 1 week after TAC. Another important consideration is the fact that *IL-6*$^{-/-}$ mice have been reported to exhibit smaller HW and HW/BW ratio with body weights of *IL-6*$^{-/-}$ starting to differ after 6 months of age.[14] Other investigators did not find differences in HW and/or HW/BW ratio at younger ages.[13,15,16] In light of these reports, and in order to avoid any potential confounding effects of *IL-6*$^{-/-}$ mice at baseline, we selected age- and body weight-matched male WT mice as controls. Importantly, our *in vivo* observations are further supported by observations in isolated cardiac myocytes (Figure 1D-G) and molecular evidence that IL-6 deletion significantly curbs the induction of genes responsible for cardiac hypertrophy (Figure 1H-J). In addition, the *in vivo* data indicating a direct role of IL-6 in pressure overload-induced hypertrophy was confirmed in our *in vitro* model of IL-6-induced

cardiac myocyte hypertrophy (Figure 7D-F). Together, these data provide conclusive evidence that IL-6 is essential for pressure overload-induced cardiac myocyte hypertrophy.

Pressure overload-induced LV remodeling, fibrosis, and failure are attenuated in the absence of IL-6

Persistent pressure overload induced by systemic hypertension or TAC results in LV hypertrophy that is preceded by diverse molecular changes and culminates in LV remodeling and eventual failure. The functional manifestation of LV remodeling is diastolic dysfunction during earlier stages and systolic impairment at later stages. Although increased IL-6 levels have been noted in patients with diastolic dysfunction,[17] no direct evidence to date has linked IL-6 to the pathogenesis of hypertensive LV remodeling and failure. Although IL-6 infusion in a previous study resulted in LV hypertrophy, blood pressure was not elevated.[4] Our results show that LV remodeling was evident in WT mice at one week after TAC. Subsequently, the LV underwent progressive hypertrophy with increasing duration of follow-up. *IL-6* deletion was beneficial in preventing LV remodeling at every stage of follow-up after TAC (Figure 2). Concentric remodeling and hypertrophy are risk factors for development of heart failure with preserved ejection fraction (HFpEF).[18] With increasing prevalence of HFpEF, it is conceivable that a strategy halting LV remodeling would prove helpful toward preventing HFpEF in patients with hypertension. Our study is the first to conclusively demonstrate that IL-6 signaling is critical toward the development of LV remodeling and failure *in vivo* in a model of pressure overload.

LV remodeling is often associated with increased myocardial fibrosis.[19] Increasing collagen deposition after persistent pressure overload or myocardial infarction contributes to the deterioration of LV compliance and development of diastolic dysfunction.[20] Our data are the first to show that *IL-6* deletion inhibits myocardial collagen deposition in both interstitial and perivascular areas after pressure overload, with greater impact on perivascular fibrosis (Figure 4A-D). These histological quantitative data were further confirmed by concordant changes in expression of fibrosis-related genes. These observations suggest that IL-6 may also play an important role in the pathogenesis of hypertensive heart failure in humans.

With regard to LV failure, elevated IL-6 levels in patients with LV dysfunction even in the absence of the clinical syndrome of congestive heart failure have been reported.[21] The current results suggest that IL-6 signaling plays an important role in the pathogenesis of LV dysfunction after pressure overload. The concordance of data from echocardiography and invasive hemodynamic studies is noteworthy in this regard. Furthermore, hemodynamic results also indicate that both LV systolic and diastolic function are preserved after TAC in mice with genetic deletion of *IL-6* (Figure 3).

IL-6 deletion attenuates cardiac myocyte apoptosis induced by pressure overload

A low level of cardiac myocyte apoptosis has been proposed as a causal mechanism for heart failure.[22] During persistent pressure overload, the molecular survival mechanisms are overwhelmed and cardiac myocyte apoptosis ensues.[23] Because of the low rate of cardiac myocyte turnover, cumulative loss of cardiac myocytes through apoptosis eventually leads to detrimental cardiac remodeling and heart failure. Although cardiac myocyte apoptosis is

commonly observed in cardiac hypertrophy, the effects of IL-6 signaling on myocyte apoptosis during cardiac hypertrophy remain unknown. A few reports have suggested that IL-6 exerts pleiotropic effects and controls the balance between anti- and pro-apoptotic pathways.[24,25] Our results from histological quantitation of apoptosis as well as molecular characterization of apoptosis regulators show that cardiac myocyte apoptosis in response to pressure overload was significantly attenuated in *IL-6*$^{-/-}$ hearts at 6 weeks after TAC (Figure 5). However, the potentially complex interactions of IL-6 signaling with cardiac myocyte apoptosis pathways during cardiac hypertrophy and failure needs to be further investigated in future studies.

Hypertrophic response is attenuated in IL-6$^{-/-}$ adult cardiac myocytes

In addition to *in vivo* experiments, we also performed mechanistic studies using adult cardiac myocytes from WT and *IL-6*$^{-/-}$ mice to examine the impact of IL-6 on cardiac myocyte hypertrophy in response to various prohypertrophic agents. Previous studies have suggested an involvement of IL-6 in inflammation and dysfunction induced by Ang II,[26] however, its role in cardiac myocyte hypertrophy triggered by common inducers of myocyte hypertrophy remains unclear. Moreover, such observations have rarely been tested in adult cardiac myocytes isolated from *IL-6*$^{-/-}$ mice. Our data show that both Ang II- and PE-induced increase in hypertrophy genes is nearly abrogated in *IL-6*$^{-/-}$ cardiac myocytes (Figure 6C,D). The necessity of IL-6 in mediation of hypertrophy in response to otherwise unrelated hypertrophy-promoting agents highlights a central role played by IL-6 in cardiac myocyte hypertrophy. Interestingly, exposure to rIL-6 produced dissimilar responses with regard to hypertrophy gene expression in *IL-6*$^{-/-}$ and WT cardiac myocytes (Figure 6A). This unexpected observation may be potentially explained by the equally unexpected finding that IL-6 receptor expression is reduced in *IL-6*$^{-/-}$ cardiac myocytes (Figure 6B).

The impact of IL-6 deletion on molecular mediators of pressure overload-induced hypertrophy

It is well known that the IL-6 family of cytokines activate JAK/STAT pathway via gp130 to mediate various cellular responses. Besides the JAK/STAT pathway, gp130 activation also leads to Akt and ERK1/2 phosphorylation. However, despite reported involvement of Akt, ERK1/2 and JNK in cardiac hypertrophy,[27] very little direct evidence exists regarding potential roles of these pathways in the context of IL-6 signaling and pressure overload. Our data from myocardial tissue samples at 6 weeks after TAC indicate that the activation of Akt, ERK, and JNK is blunted in *IL-6*$^{-/-}$ hearts, indicating broad suppression of pro-hypertrophy signaling in the absence of IL-6. Furthermore, we noted increased phosphorylation of GSK-3β in WT hearts at 6 weeks after TAC, which was abrogated in *IL-6*$^{-/-}$ hearts (Online Figure IIID,F). To our knowledge, this is the first evidence that phosphorylation and inhibition of GSK-3β in the setting of pressure overload requires intact IL-6 signaling.

With regard to STAT3, published evidence indicates that members of ‘IL-6 family’ are able to induce cardiac myocyte hypertrophy via gp130-mediated STAT3 activation. However, published evidence directly implicating IL-6 in this process is sparse and inconclusive. Moreover, in the study by Lai et al., myocardial STAT3 activation was not affected in *IL-6*$^{-/-}$ mice after TAC.[6] Our results show that STAT3 activation was markedly attenuated in

the absence of IL-6 at 6 weeks after TAC (Figure 7A,B). This is consistent with the paradigm that IL-6 itself plays an important and non-redundant role in pressure overload-induced activation of STAT3. These data also suggest that the absence of IL-6 is not functionally compensated by upregulation of other members of IL-6 family. In conjunction with the *in vitro* data with Ang II and PE stimulation, these results identify a central role of STAT3 activation during pressure overload.

The role of CaMKII in IL-6-induced STAT3 activation and cardiac myocyte hypertrophy

CaMKII is known to play an important role during cardiac hypertrophy.[28] Although CaMKII is upregulated after pressure overload,[29] whether CaMKII plays any role in IL-6-induced cardiac hypertrophy remains unknown. Moreover, the participation of CaMKII signaling in heart failure is complex and may vary depending on etiology[30] and other associated pathologies, such as diabetes.[31] Our results show that myocardial p-CaMKII levels are markedly elevated in WT mice at 6 weeks after TAC, and this increase is abrogated in the absence of IL-6 (Figure 8A,C). Furthermore, the time-dependent increase in p-CaMKII levels in H9c2 cells following rIL-6 exposure confirmed the ability of IL-6 to directly activate CaMKII. Consistently, IL-6-induced increase in cell surface area and hypertrophy gene induction was blocked by inhibition of CaMKII, indicating a critical role of this kinase.

Interestingly, the time-course of CaMKII activation was very similar to STAT3 activation following IL-6 stimulation *in vitro*. When KN-62, a CaMKII inhibitor, was added in addition to IL-6, the inhibition of STAT3 activation was also mirrored changes in p-CaMKII levels, indicating that inhibition of CaMKII activation prevents STAT3 activation in response to IL-6. These results were further confirmed in assays using cytoplasmic and nuclear protein fractions. To our knowledge, these results from *in vivo* as well as *in vitro* experiments provide the first evidence that CaMKII is necessary for the activation of STAT3 by IL-6. These data also identify CaMKII as an essential component of IL-6 signaling toward inducing cardiac hypertrophy in response to pressure overload.

CONCLUSIONS

The current findings provide definitive evidence that IL-6 signaling is critically important toward the development of LV hypertrophy, remodeling and dysfunction during pressure overload. Our results also identify a heretofore unknown role of CaMKII in IL-6-induced STAT3 activation and cardiac myocyte hypertrophy. These insights may be utilized to formulate novel pharmacological approaches to ameliorate hypertensive heart disease.

Supplementary Material

Refer to Web version on PubMed Central for supplementary material.

Acknowledgments

SOURCES OF FUNDING

This work was supported in part by National Institutes of Health grant R01 HL-117730.

Nonstandard Abbreviations and Acronyms

IL-6$^{-/-}$	*Interleukin-6* knock out
WT	wild type
CaMKII	Ca^{2+}/calmodulin-dependent protein kinase II
STAT3	signal transducer and activator of transcription 3
LV	left ventricle
TAC	transverse aortic constriction
HW/TL	heart weight/tibia length
HW/BW	heart weight/body weight
LVEDD	LV end-diastolic diameter
LVEDV	LV end-diastolic volume
EF	ejection fraction
FS	fraction shortening
LVESV	LV end-systolic volume
LVEDP	LV end-diastolic pressure
Ang II	angiotensin II
PE	phenylephrine
NE	norepinephrine

REFERENCES

1. Hunter CA, Jones SA. IL-6 as a keystone cytokine in health and disease. Nat Immunol. 2015; 16:448–457. [PubMed: 25898198]
2. Kukielka GL, Smith CW, Manning AM, Youker KA, Michael LH, Entman ML. Induction of interleukin-6 synthesis in the myocardium. Potential role in postreperfusion inflammatory injury. Circulation. 1995; 92:1866–1875. [PubMed: 7671371]
3. Hirota H, Yoshida K, Kishimoto T, Taga T. Continuous activation of gp130, a signal-transducing receptor component for interleukin 6-related cytokines, causes myocardial hypertrophy in mice. Proc Natl Acad Sci U S A. 1995; 92:4862–4866. [PubMed: 7539136]
4. Melendez GC, McLarty JL, Levick SP, Du Y, Janicki JS, Brower GL. Interleukin 6 mediates myocardial fibrosis, concentric hypertrophy, and diastolic dysfunction in rats. Hypertension. 2010; 56:225–231. [PubMed: 20606113]
5. Kaminski KA, Oledzka E, Bialobrzewska K, Kozuch M, Musial WJ, Winnicka MM. The effects of moderate physical exercise on cardiac hypertrophy in interleukin 6 deficient mice. Adv Med Sci. 2007; 52:164–168. [PubMed: 18217411]
6. Lai NC, Gao MH, Tang E, Tang R, Guo T, Dalton ND, Deng A, Tang T. Pressure overload-induced cardiac remodeling and dysfunction in the absence of interleukin 6 in mice. Lab Invest. 2012; 92:1518–1526. [PubMed: 22825686]

7. Dawn B, Guo Y, Rezazadeh A, Huang Y, Stein AB, Hunt G, Tiwari S, Varma J, Gu Y, Prabhu SD, Kajstura J, Anversa P, Ildstad ST, Bolli R. Postinfarct cytokine therapy regenerates cardiac tissue and improves left ventricular function. Circ Res. 2006; 98:1098–1105. [PubMed: 16556872]
8. Dawn B, Tiwari S, Kucia MJ, Zuba-Surma EK, Guo Y, Sanganalmath SK, Abdel-Latif A, Hunt G, Vincent RJ, Taher H, Reed NJ, Ratajczak MZ, Bolli R. Transplantation of bone marrow-derived very small embryonic-like stem cells attenuates left ventricular dysfunction and remodeling after myocardial infarction. Stem Cells. 2008; 26:1646–1655. [PubMed: 18420834]
9. Kunisada K, Tone E, Fujio Y, Matsui H, Yamauchi-Takihara K, Kishimoto T. Activation of gp130 transduces hypertrophic signals via STAT3 in cardiac myocytes. Circulation. 1998; 98:346–352. [PubMed: 9711940]
10. Uozumi H, Hiroi Y, Zou Y, Takimoto E, Toko H, Niu P, Shimoyama M, Yazaki Y, Nagai R, Komuro I. gp130 plays a critical role in pressure overload-induced cardiac hypertrophy. J Biol Chem. 2001; 276:23115–23119. [PubMed: 11262406]
11. Saito T, Fukuzawa J, Osaki J, Sakuragi H, Yao N, Haneda T, Fujino T, Wakamiya N, Kikuchi K, Hasebe N. Roles of calcineurin and calcium/calmodulin-dependent protein kinase II in pressure overload-induced cardiac hypertrophy. J Mol Cell Cardiol. 2003; 35:1153–1160. [PubMed: 12967638]
12. Meier H, Bullinger J, Marx G, Deten A, Horn LC, Rassler B, Zimmer HG, Briest W. Crucial role of interleukin-6 in the development of norepinephrine-induced left ventricular remodeling in mice. Cell Physiol Biochem. 2009; 23:327–3341. [PubMed: 19471100]
13. Coles B, Fielding CA, Rose-John S, Scheller J, Jones SA, O'Donnell VB. Classic interleukin-6 receptor signaling and interleukin-6 trans-signaling differentially control angiotensin II-dependent hypertension, cardiac signal transducer and activator of transcription-3 activation, and vascular hypertrophy in vivo. Am J Pathol. 2007; 171:315–325. [PubMed: 17591976]
14. Wallenius V, Wallenius K, Ahren B, Rudling M, Carlsten H, Dickson SL, Ohlsson C, Jansson JO. Interleukin-6-deficient mice develop mature-onset obesity. Nat Med. 2002; 8:75–79. [PubMed: 11786910]
15. Dawn B, Xuan YT, Guo Y, Rezazadeh A, Stein AB, Hunt G, Wu WJ, Tan W, Bolli R. IL-6 plays an obligatory role in late preconditioning via JAK-STAT signaling and upregulation of iNOS and COX-2. Cardiovasc Res. 2004; 64:61–71. [PubMed: 15364614]
16. Fuchs M, Hilfiker A, Kaminski K, Hilfiker-Kleiner D, Guener Z, Klein G, Podewski E, Schieffer B, Rose-John S, Drexler H. Role of interleukin-6 for LV remodeling and survival after experimental myocardial infarction. Faseb j. 2003; 17:2118–2120. [PubMed: 12958147]
17. Dinh W, Futh R, Nickl W, Krahn T, Ellinghaus P, Scheffold T, Bansemir L, Bufe A, Barroso MC, Lankisch M. Elevated plasma levels of TNF-alpha and interleukin-6 in patients with diastolic dysfunction and glucose metabolism disorders. Cardiovasc Diabetol. 2009; 8:58. [PubMed: 19909503]
18. Paulus WJ, Tschope C. A novel paradigm for heart failure with preserved ejection fraction: comorbidities drive myocardial dysfunction and remodeling through coronary microvascular endothelial inflammation. J Am Coll Cardiol. 2013; 62:263–271. [PubMed: 23684677]
19. Sutton MG, Sharpe N. Left ventricular remodeling after myocardial infarction: pathophysiology and therapy. Circulation. 2000; 101:2981–2988. [PubMed: 10869273]
20. Kasner M, Westermann D, Lopez B, Gaub R, Escher F, Kuhl U, Schultheiss HP, Tschope C. Diastolic tissue Doppler indexes correlate with the degree of collagen expression and cross-linking in heart failure and normal ejection fraction. J Am Coll Cardiol. 2011; 57:977–985. [PubMed: 21329845]
21. Raymond RJ, Dehmer GJ, Theoharides TC, Deliargyris EN. Elevated interleukin-6 levels in patients with asymptomatic left ventricular systolic dysfunction. Am Heart J. 2001; 141:435–438. [PubMed: 11231442]
22. Wencker D, Chandra M, Nguyen K, Miao W, Garantziotis S, Factor SM, Shirani J, Armstrong RC, Kitsis RN. A mechanistic role for cardiac myocyte apoptosis in heart failure. J Clin Invest. 2003; 111:1497–1504. [PubMed: 12750399]
23. Diwan A, Dorn GW 2nd. Decompensation of cardiac hypertrophy: cellular mechanisms and novel therapeutic targets. Physiology (Bethesda). 2007; 22:56–64. [PubMed: 17289931]

24. Scheller J, Chalaris A, Schmidt-Arras D, Rose-John S. The pro- and anti-inflammatory properties of the cytokine interleukin-6. Biochim Biophys Acta. 2011; 1813:878–888. [PubMed: 21296109]
25. Wollert KC, Drexler H. The role of interleukin-6 in the failing heart. Heart Fail Rev. 2001; 6:95–103. [PubMed: 11309528]
26. Gonzalez GE, Rhaleb NE, D'Ambrosio MA, Nakagawa P, Liu Y, Leung P, Dai X, Yang XP, Peterson EL, Carretero OA. Deletion of interleukin-6 prevents cardiac inflammation, fibrosis and dysfunction without affecting blood pressure in angiotensin II-high salt-induced hypertension. J Hypertens. 2015; 33:144–152. [PubMed: 25304471]
27. Clerk A, Sugden PH. Activation of protein kinase cascades in the heart by hypertrophic G protein-coupled receptor agonists. Am J Cardiol. 1999; 83:64h–69h.
28. Anderson ME, Brown JH, Bers DM. CaMKII in myocardial hypertrophy and heart failure. J Mol Cell Cardiol. 2011; 51:468–473. [PubMed: 21276796]
29. Colomer JM, Mao L, Rockman HA, Means AR. Pressure overload selectively up-regulates Ca2+/calmodulin-dependent protein kinase II in vivo. Mol Endocrinol. 2003; 17:183–192. [PubMed: 12554746]
30. Netticadan T, Temsah RM, Kawabata K, Dhalla NS. Sarcoplasmic reticulum Ca(2+)/Calmodulin-dependent protein kinase is altered in heart failure. Circ Res. 2000; 86:596–605. [PubMed: 10720422]
31. Netticadan T, Temsah RM, Kent A, Elimban V, Dhalla NS. Depressed levels of Ca2+-cycling proteins may underlie sarcoplasmic reticulum dysfunction in the diabetic heart. Diabetes. 2001; 50:2133–2138. [PubMed: 11522681]

Novelty and Significance

What Is Known?

- Interleukin (IL)-6 has been implicated in several cardiovascular pathologies.
- IL-6 has been shown to induce cardiac myocyte hypertrophy, without increasing blood pressure; however, published reports also indicate that IL-6 is not essential for left ventricular (LV) hypertrophy.
- The role of IL-6 in pressure overload-induced cardiac hypertrophy and failure remains controversial and the underlying molecular signaling poorly understood.

What New Information Does This Article Contribute?

- Genetic deletion of *IL-6* attenuates LV hypertrophy and remodeling induced by pressure overload *in vivo* and prevents cardiac myocyte hypertrophy *in vitro* following exposure to hypertrophy-promoting agents, indicating an essential role of IL-6 in cardiac myocyte hypertrophy.
- Cardiac myocyte apoptosis and LV dysfunction in response to pressure overload are attenuated in the absence of IL-6.
- Ca^{2+}/calmodulin-dependent protein kinase II (CaMKII) plays an important role in IL-6-induced STAT3 activation and consequent cardiac myocyte hypertrophy during pressure overload, and GSK-3β inhibition in the setting of pressure overload requires intact IL-6 signaling.

IL-6, a pleiotropic cytokine with multi-faceted actions, has been implicated in cardiac hypertrophy; however, the precise role of IL-6 in this process remains unclear. . Our echocardiographic and hemodynamic data show that LV hypertrophy, remodeling, and dysfunction in response to pressure overload induced by transverse aortic constriction *in vivo* are ameliorated in mice with genetic deletion of *IL-6*. These physiological changes are accompanied by reduced myocardial fibrosis and apoptosis at the tissue level. The necessity of IL-6 for cardiomyocyte hypertrophy is further evidenced by blunted enlargement of IL-6-deficient cardiomyocytes following stimulation with hypertrophy-promoting agents. The current data also provide evidence that CaMKII is necessary for the activation of STAT3 by IL-6 in the setting of pressure overload; and suggest that IL-6 signaling is important in phosphorylation and inhibition of GSK-3β. These findings suggest that IL-6 signaling is critical for ventricular hypertrophy and dysfunction during pressure overload. Thus, therapeutic modulation of IL-6 signaling could potentially benefit patients with hypertensive heart disease.

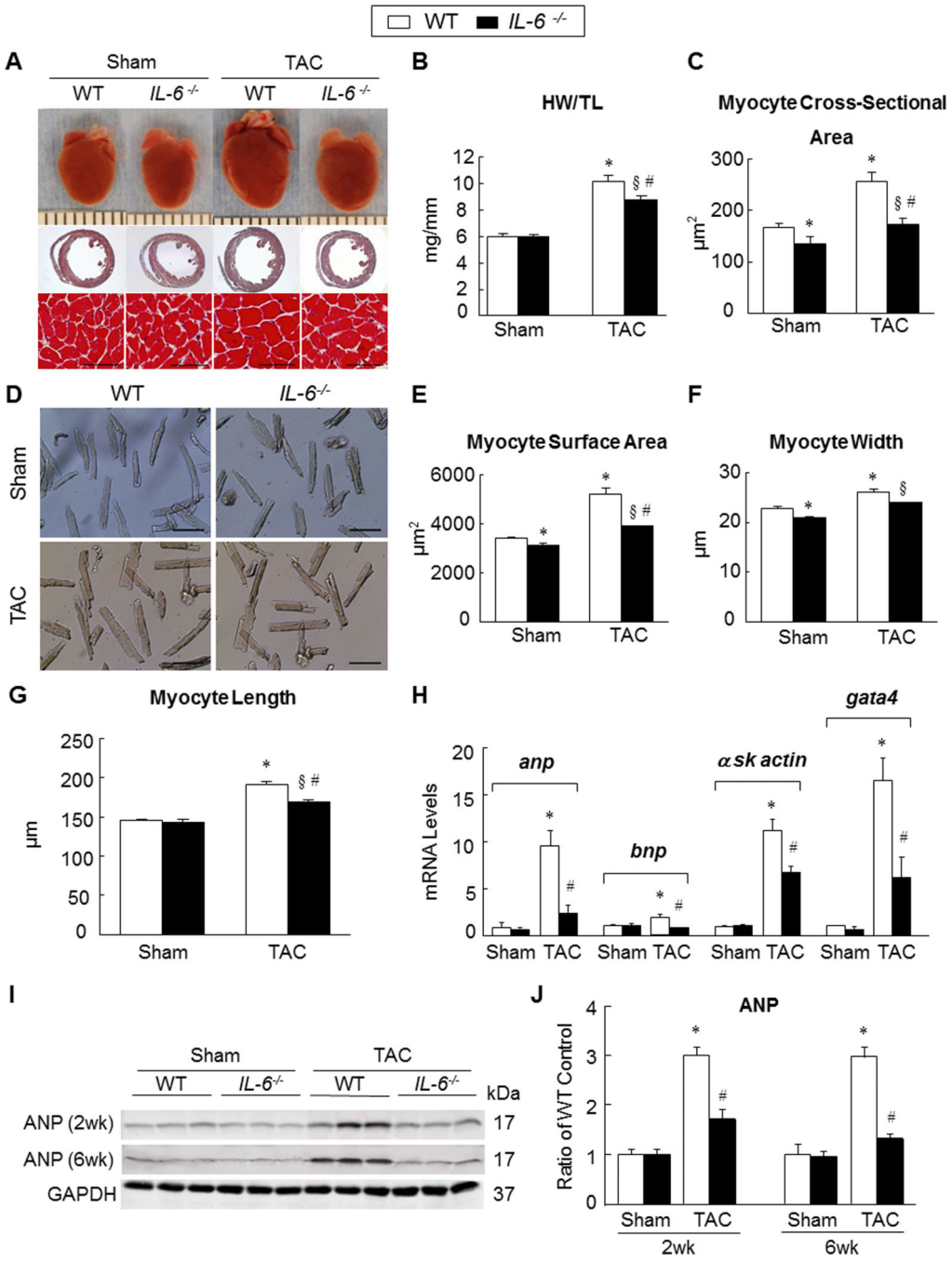

Figure 1. Genetic deletion of *IL-6* attenuated LV hypertrophy induced by pressure overload *in vivo*

A, representative images showing gross cardiac morphology used for HW/TL calculation (upper panel); transverse sections stained with Masson's trichrome (middle panel); microscopic cross-sections stained with Masson's trichrome and used for calculation of transverse myocyte area (lower panel), scale bars, 50μm (n=10-12 per group). **B-C,** bar graphs showing quantitative data for HW/TL (**B**) and myocyte cross sectional area (**C**) (n=10-12 per group). **D,** representative images of isolated cardiac myocytes used for the

assessment of myocyte cell surface area, myocyte width and myocyte length, scale bars, 100μm. **E,** Quantitative assessment of myocyte cell surface area calculated from isolated cardiac myocytes (n=6 per group). **F,** Myocyte width calculated from isolated cardiac myocytes (n=6 per group). **G,** Myocyte length calculated from isolated cardiac myocytes (n=6 per group). **H,** Transcriptional profiling of cardiac hypertrophy-related genes using qRT-PCR at 2 weeks after surgery (n=6 per group). **I** and **J,** representative western blots with quantification showing expression of ANP in WT and *IL-6*$^{-/-}$ mice at 2 and 6 weeks after surgery (n=6 per group). Data represent means ± SEM. **P*<0.05 vs. Sham WT mice; § *P*<0.05 vs. Sham *IL-6*$^{-/-}$ mice; # *P*<0.05 vs. TAC WT mice.

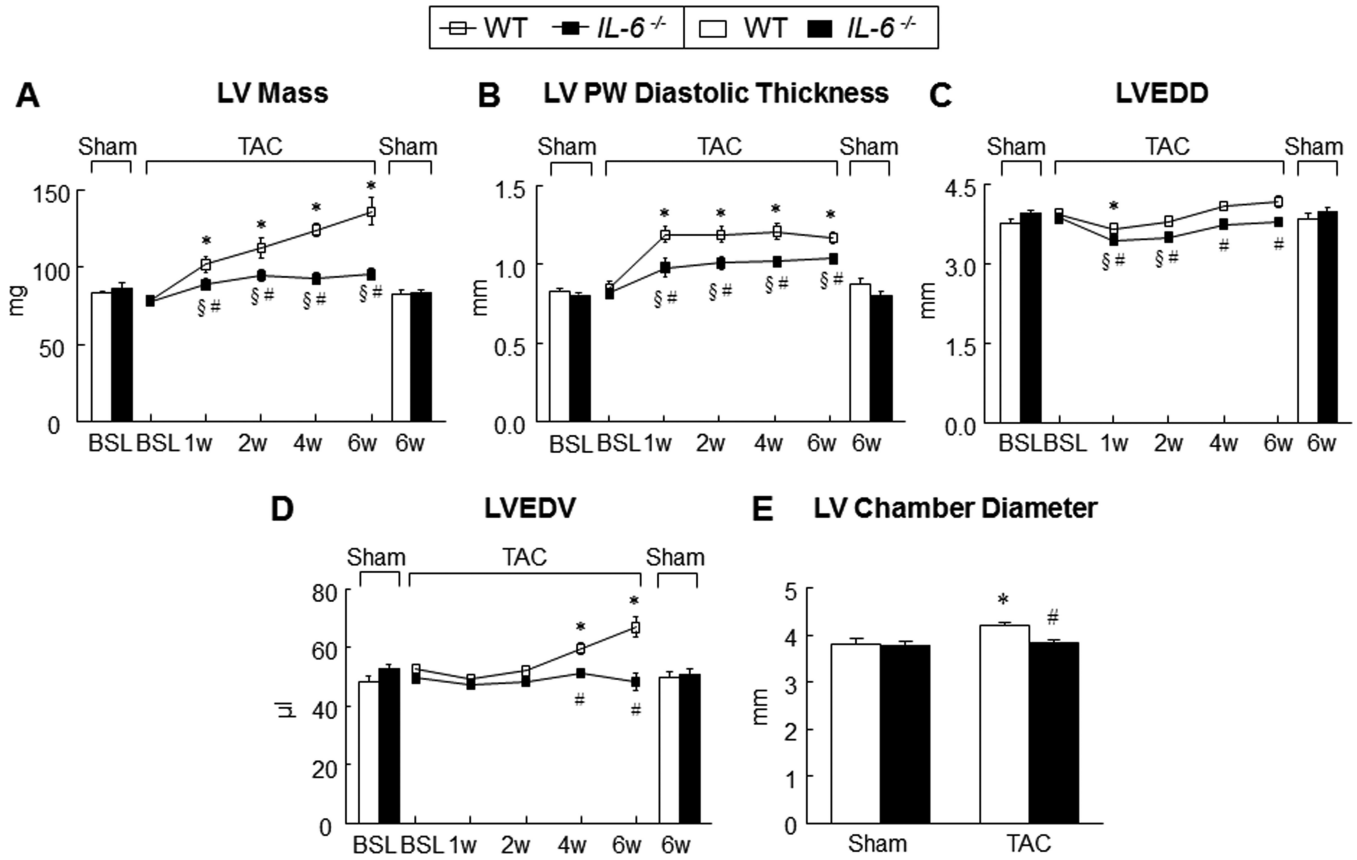

Figure 2. Genetic deletion of *IL-6* prevented adverse remodeling induced by pressure overload

The parameters of LV remodeling were assessed using serial echocardiography and histological sections of harvested hearts arrested in diastole. **A-D,** serial echocardiographic quantitative data on LV mass (**A**), LV posterior wall end-diastolic thickness (**B**), LVEDD (**C**), and LVEDV (**D**); **P*<0.05 vs. baseline (BSL) in TAC WT mice; § *P*<0.05 vs. BSL in TAC *IL-6*$^{-/-}$ mice; # *P*<0.05 vs TAC WT mice. **E,** myocardial sections from hearts arrested in end-diastole were used to calculate LV chamber size at 6 weeks after surgery. Data represent means ± SEM. **P*<0.05 vs sham WT mice; # *P*<0.05 vs TAC WT mice. A-D, there was no statistically significant difference at baseline among Sham and TAC groups of WT and *IL-6*$^{-/-}$ mice.

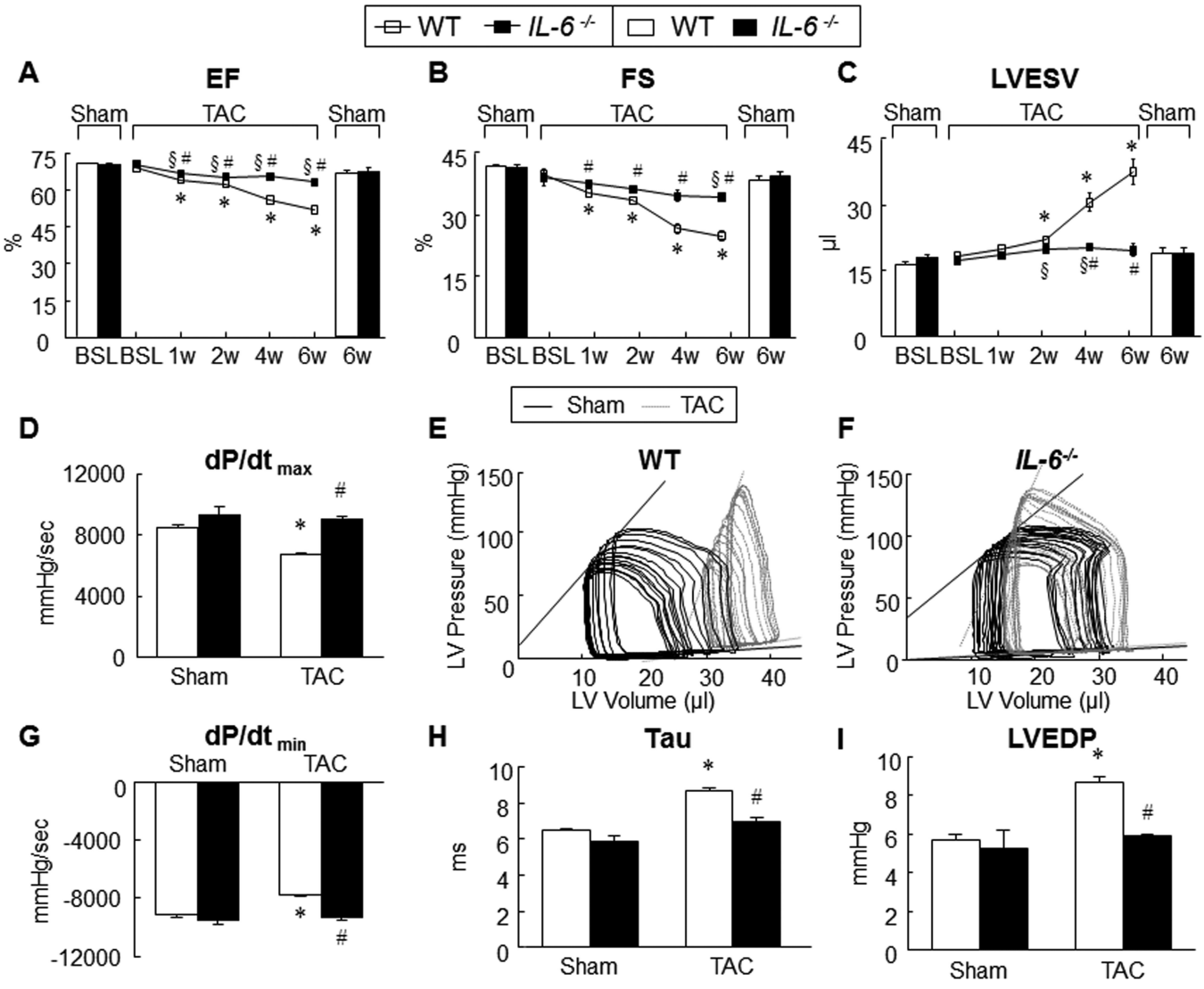

Figure 3. Genetic deletion of IL-6 ameliorated cardiac dysfunction induced by pressure overload

A-C, LVEF, LVFS and LVESV were assessed by serial echocardiography in WT and *IL-6*$^{-/-}$ mice before and at 1, 2, 4 and 6 weeks after surgery (n=10-12 mice per group), **P*<0.05 vs. BSL in TAC WT mice; § *P*<0.05 vs. BSL in TAC *IL-6*$^{-/-}$ mice, # *P*<0.05 vs. TAC WT mice. **D,** LV systolic function represented by LV contractility index (dP/dt_{max}) as assessed during invasive hemodynamics at 6 weeks after surgery (n=10-12 mice per group). **E** and **F,** representative LV pressure-volume loops from WT and *IL-6*$^{-/-}$ mice (loops from sham-operated animal are shown in black and those from TAC-operated in grey) at 6 weeks after surgery. ESPVR is represented by the line joining end-systolic pressure and volume coordinates. **G** and **H,** LV diastolic function represented by speed of cardiac relaxation (dP/dt_{min}) and relaxation constant (tau) as assessed by invasive hemodynamic studies at 6 weeks after surgery (n=10-12 mice per group). **I,** LV end-diastolic pressure (LVEDP) assessed during invasive hemodynamic study at 6 weeks after surgery (n=10-12 mice per group). **P*<0.05 vs. Sham WT mice; # *P*<0.05 vs. TAC WT mice.

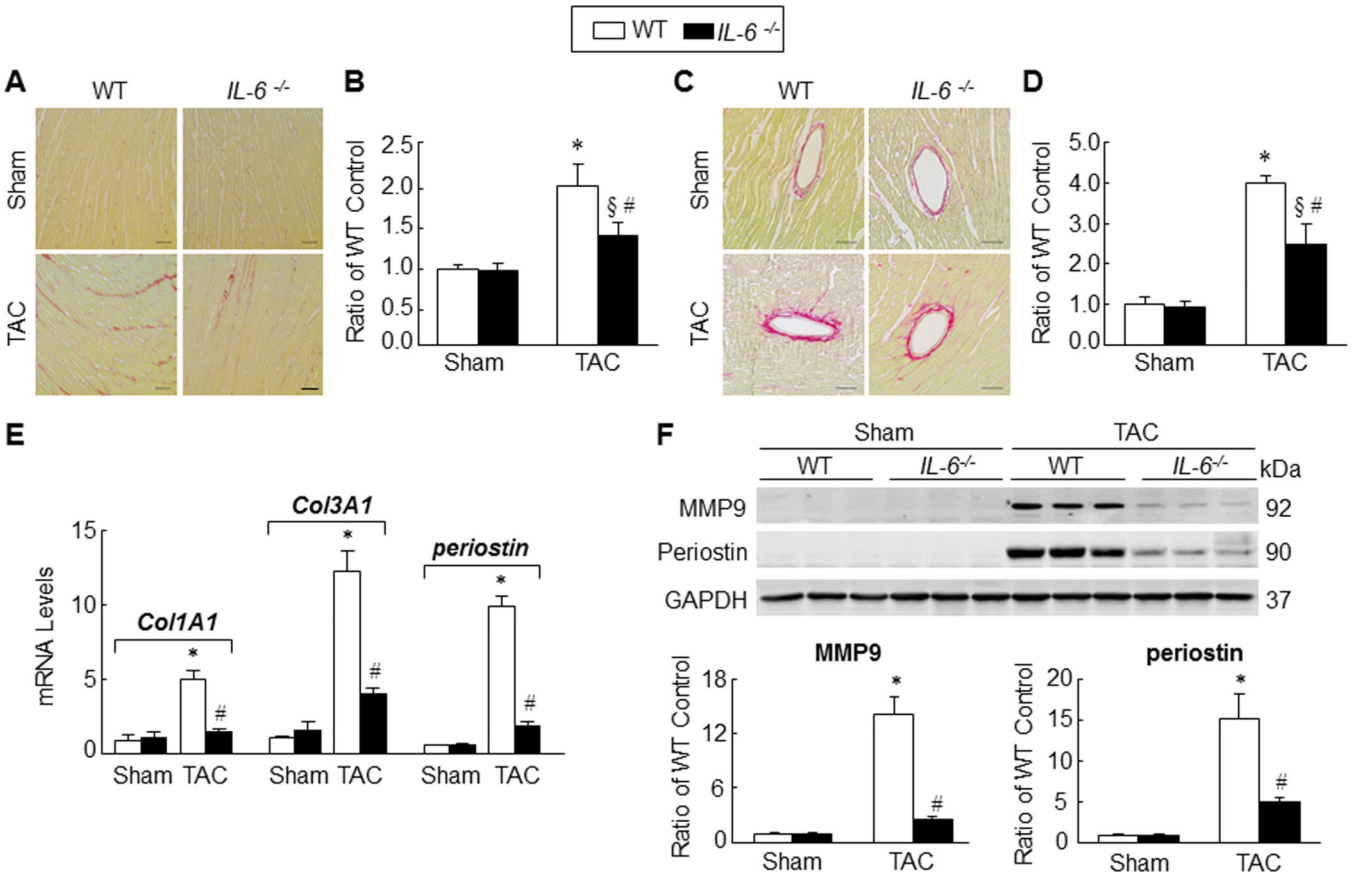

Figure 4. Genetic deletion of *IL-6* attenuated pressure overload-induced LV fibrosis

Myocardial fibrosis was quantitated in picrosirius red-stained myocardial sections from WT and *IL-6*$^{-/-}$ mouse hearts at 6 weeks after surgery. **A-D,** representative images and quantification of interstitial (**A** and **B**) and perivascular fibrosis (**C** and **D**), scale bar, 50μm (n=9-14 mice per group). **E,** mRNA levels of *Col1A1*, *Col3A1* and *periostin* were analyzed by qPCR from WT and *IL-6*$^{-/-}$ mouse hearts at 2 weeks after surgery. The relative abundance of transcripts were quantified and normalized to GAPDH (n=6 per group). **F,** representative Western immunoblots and quantitation of MMP9 and periostin protein levels from WT and *IL-6*$^{-/-}$ mouse hearts at 6 weeks after surgery (n=6 per group). Data represent means ± SEM. *P<0.05 vs. Sham WT mice; § P<0.05 vs. Sham *IL-6*$^{-/-}$ mice; # P<0.05 vs. TAC WT mice.

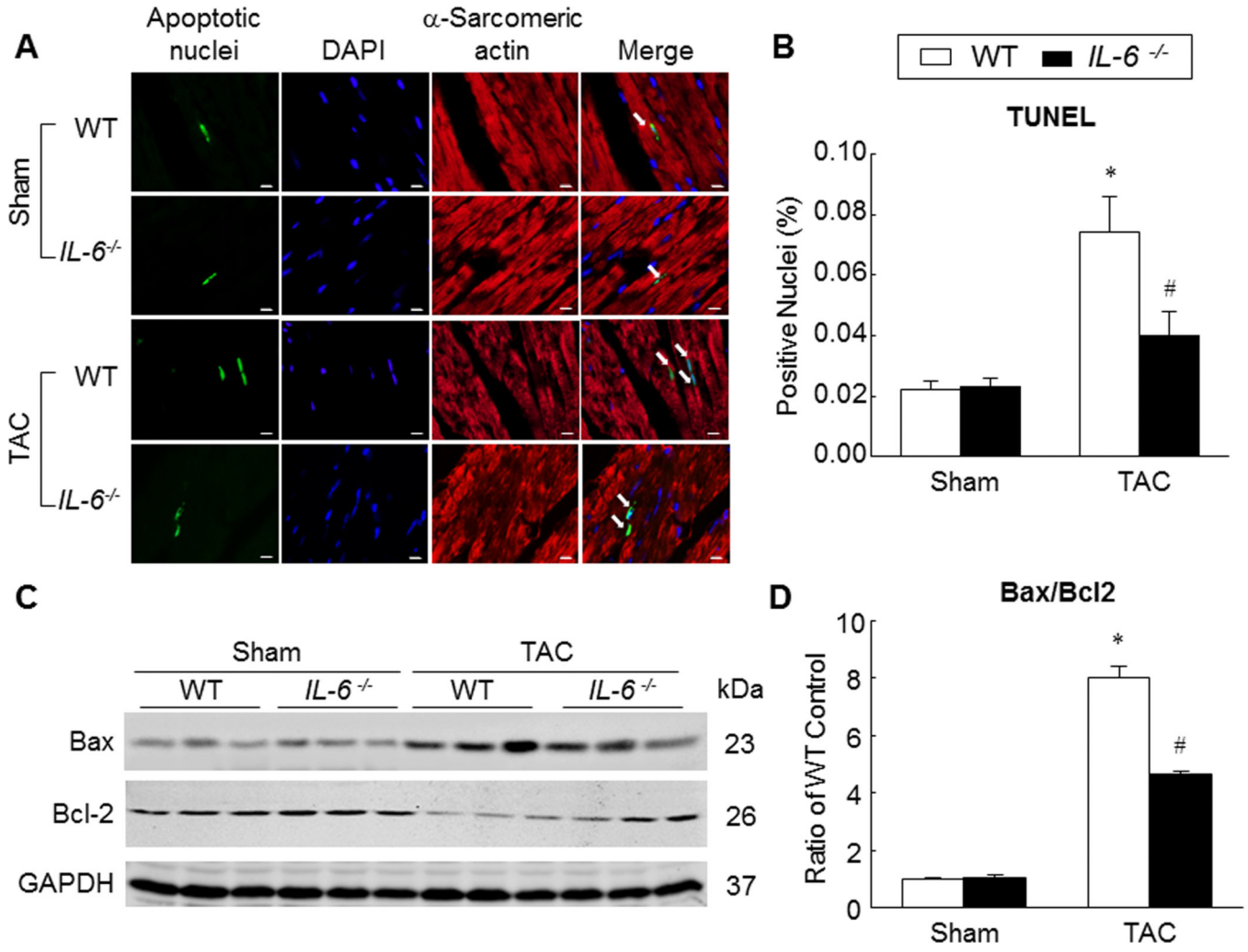

Figure 5. Attenuation of pressure overload-induced cardiac myocyte apoptosis in the absence of IL-6

A and **B,** TUNEL staining was performed on myocardial sections from WT and *IL-6*$^{-/-}$ hearts harvested at 6 weeks after surgery. Apoptotic nuclei (white arrows) are visualized by green fluorescence. Nuclei are identified in blue (DAPI). Sections were co-immunostained with anti-α-sarcomeric actin (red) to identify cardiac myocytes. TUNEL-positive myocyte nuclei were quantitated as a percentage of total cardiac myocyte nuclei, scale bar, 5μm (n=10-12 per group). **C,** representative Western immunoblots for Bax and Bcl-2. **D,** bar graph showing the ratio of Bax to Bcl-2 (n=6 per group). Data represent means ± SEM. **P*<0.05 vs. Sham WT mice; # *P*<0.05 vs. TAC WT mice.

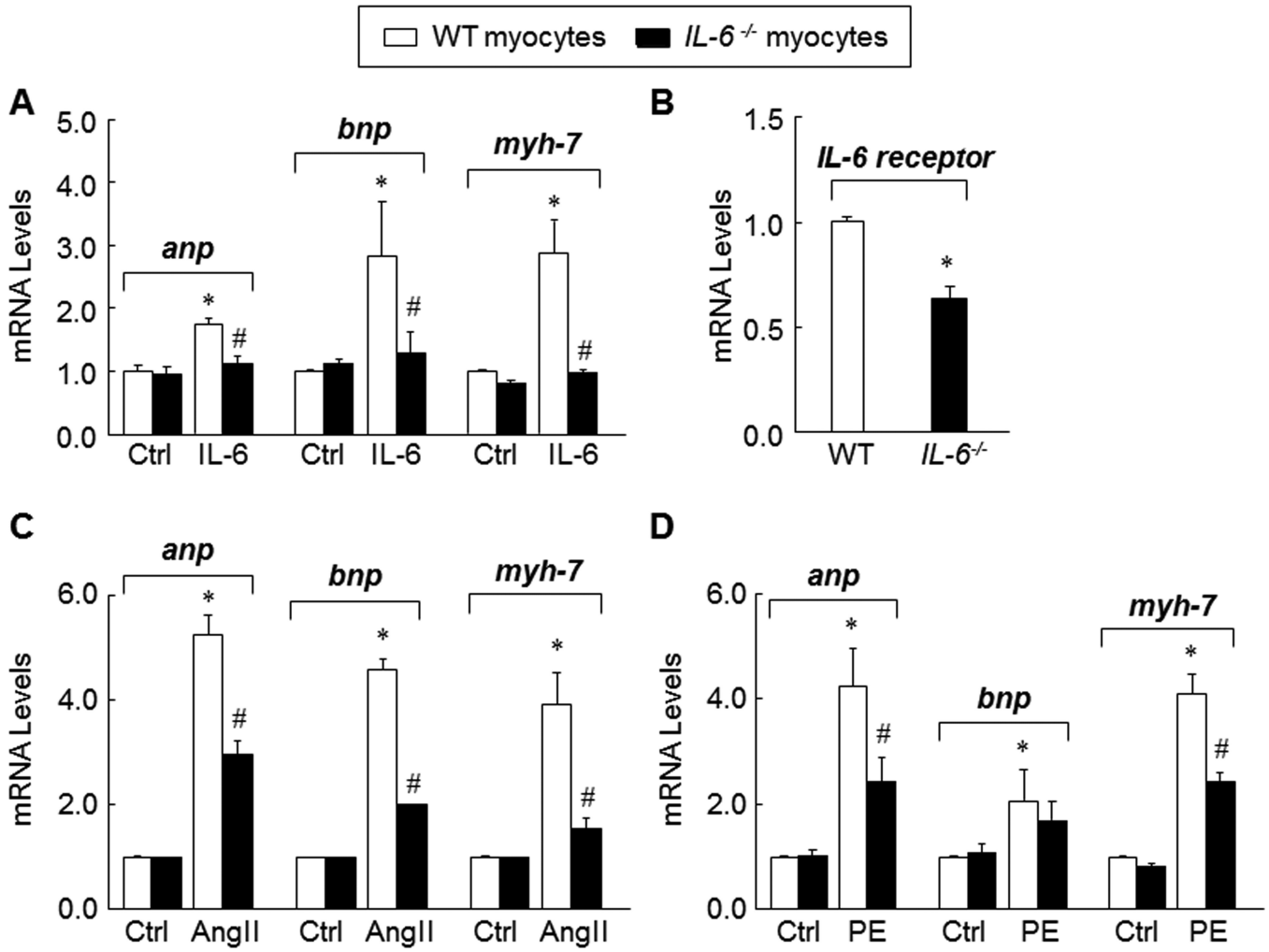

Figure 6. Requirement of IL-6 for adult cardiac myocyte hypertrophy

A, expression of hypertrophy-related genes (*anp*, *bnp* and *myh-7*) in adult mouse cardiac myocytes from WT and *IL-6*$^{-/-}$ mice following stimulation with rIL-6 (50ng/ml) for 24 h. **B,** expression of IL-6 receptor in WT and *IL-6*$^{-/-}$ cardiac myocytes. **C,** expression of *anp*, *bnp* and *myh-7* in adult cardiac myocytes from WT and *IL-6*$^{-/-}$ mice following stimulation with Ang II (1×10^{-7} mol/L) for 48 h. **D,** expression of *anp*, *bnp* and *myh-7* in adult cardiac myocytes from WT and *IL-6*$^{-/-}$ mice following stimulation with PE (10μmol/L) for 24 h. Data represent mean ± SEM from three independent experiments. **P*<0.05 vs. WT cardiac myocytes; #*P*<0.05 vs. WT cardiac myocytes treated with pro-hypertrophic stimulators.

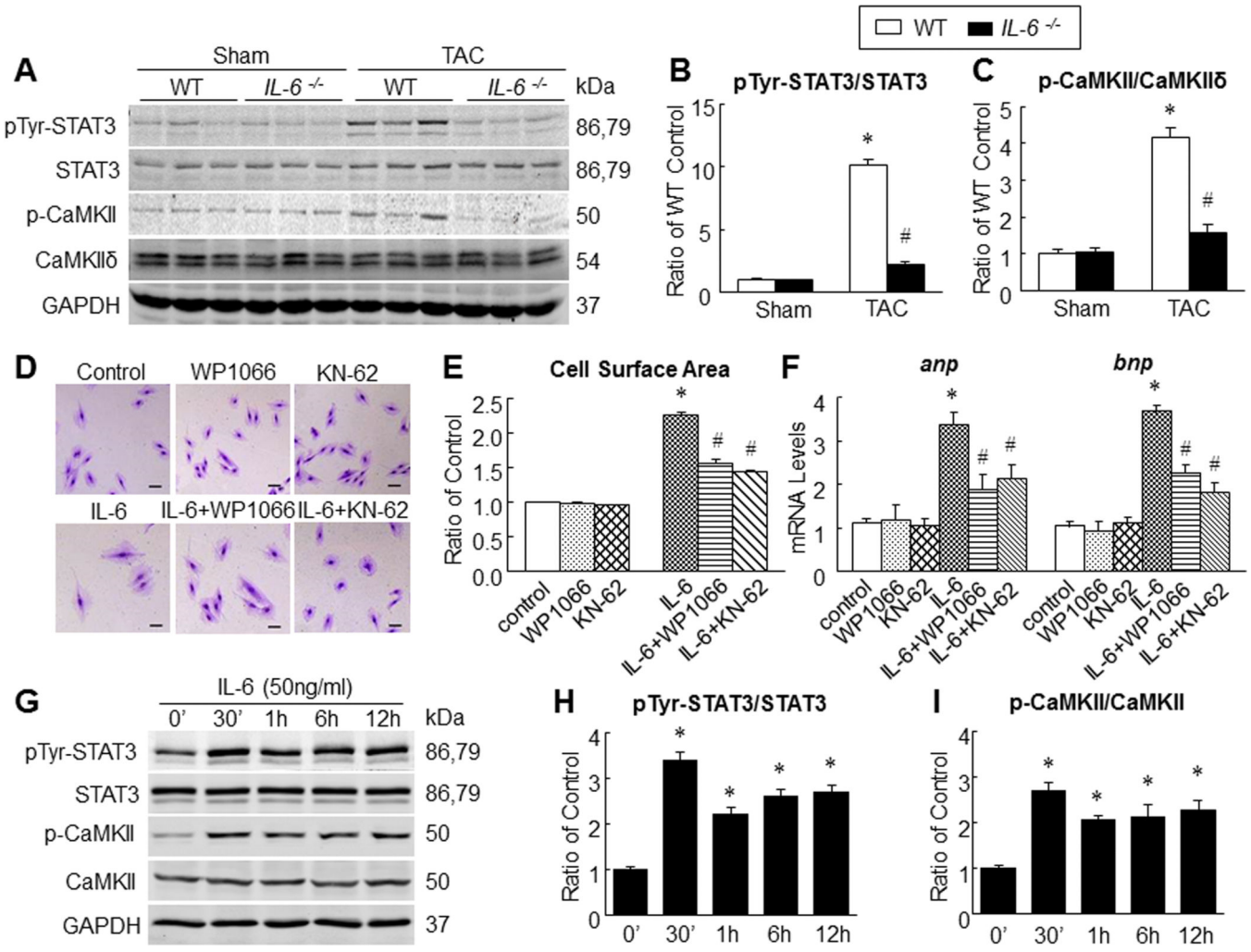

Figure 7. STAT3 and CaMKII contributed to IL-6-Induced cardiac myocyte hypertrophy

A-C, representative Western immunoblots (**A**) and quantitative data for pTyr-STAT3 (**B**) and p-CaMKII (**C**) in WT and *IL-6*$^{-/-}$ mouse hearts at 6 weeks after surgery (n=6 per group), **P*<0.05 vs. Sham WT mice; #*P*<0.05 vs. TAC WT mice. **D,** representative images of H9c2 cells stained with 1% crystal violet after treatment with KN-62 (10μmol/L) or WP1066 (6μmol/L) in the presence and absence of rIL-6 (50ng/ml) for 24 h, scale bar=100 μm. **E,** cell surface area measured after 24 h of exposure to rIL-6 in the presence or absence of inhibitors of CaMKII or STAT3. **F,** Levels of mRNA for *anp* and *bnp* as determined by qPCR after 24 h of exposure to rIL-6 in the presence or absence of inhibitors of CaMKII and STAT3. (**GI**) stimulation with rIL-6 (50ng/ml) for variable duration with subsequent quantitation of pTyr-STAT3 (**H**) and p-CaMKII (**I**). Data represent means ± SEM from three independent experiments. **P*<0.05 vs. control; # *P*<0.05 vs. rIL-6 treatment only.

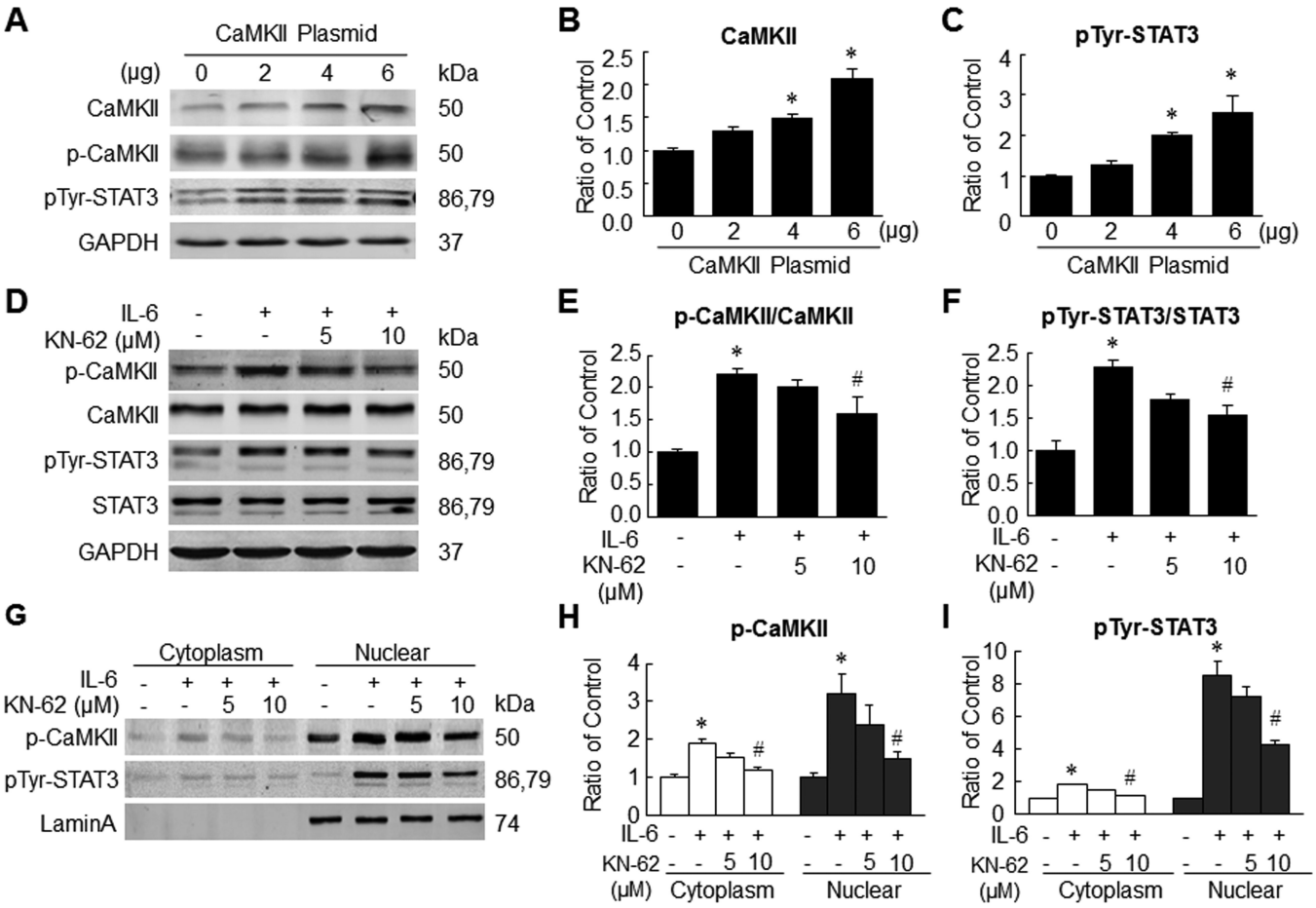

Figure 8. IL-6-induced STAT3 phosphorylation and translocation in part via a CaMKII-dependent manner

A-C, H9c2 cells were transfected with 2, 4 and 6 μg of plasmids encoding CaMKII. Representative Western immunoblots (**A**) and quantitative data for CaMKII (**B**) and pTyr-STAT3 (**C**). **D-F,** representative Western immunoblots (**D**) and quantitative data for p-CaMKII (**E**) and pTyr-STAT3 (**F**) after stimulation with rIL-6 (50ng/ml) in the presence or absence of KN-62 (5μmol/L or 10μmol/L). **G-I,** representative Western immunoblots (**G**) and quantitative data for cytoplasmic and nuclear contents of p-CaMKII (**H**) and pTyr-STAT3 (**I**) after stimulation with rIL-6 (50ng/ml) in the presence or absence of KN-62 (5μmol/L or 10μmol/L). Data represent means ± SEM from three independent experiments. **P*<0.05 vs. control; # *P*<0.05 vs. IL-6 treatment only.